Molecular Therapy
Nucleic Acids
Original Article

miR-424/322 protects against abdominal aortic aneurysm formation by modulating the Smad2/3/runt-related transcription factor 2 axis

Hsiao-Ya Tsai,[1] Jen-Chun Wang,[1,2] Yu-Juei Hsu,[3] Yi-Lin Chiu,[6] Chih-Yuan Lin,[4] Cheng-Yo Lu,[1] and Shih-Hung Tsai[1,5]

[1]Department of Emergency Medicine, Tri-Service General Hospital, National Defense Medical Center, No. 325, Section 2, Cheng-Kung Road, Neihu District, Taipei 11490, Taiwan; [2]Institute of Clinical Medicine, National Yang-Ming University, Taipei, Taiwan; [3]Division of Nephrology, Department of Internal Medicine, Tri-Service General Hospital, National Defense Medical Center, Taipei, Taiwan; [4]Department of Surgery, Division of Cardiovascular Surgery, Tri-Service General Hospital, National Defense Medical Center, Taipei, Taiwan; [5]Department of Physiology and Biophysics, Graduate Institute of Physiology, National Defense Medical Center, Taipei, Taiwan; [6]Department of Biochemistry, National Defense Medical Center, Taipei, Taiwan

Rupture of abdominal aortic aneurysms (AAAs) is one of the leading causes of sudden death in the elderly population. The osteogenic transcription factor runt-related gene (RUNX) encodes multifunctional mediators of intracellular signal transduction pathways in vascular remodeling and inflammation. We aimed to evaluate the roles of RUNX2 and its putative downstream target miR-424/322 in the modulation of several AAA progression-related key molecules, such as matrix metalloproteinases and vascular endothelial growth factor. In the GEO database, we found that male patients with AAAs had higher RUNX2 expression than did control patients. Several risk factors for aneurysm induced the overexpression of MMPs through RUNX2 transactivation, and this was dependent on Smad2/3 upregulation in human aortic smooth muscle cells. miR-424 was overexpressed through RUNX2 after angiotensin II (AngII) challenge. The administration of siRUNX2 and miR-424 mimics attenuated the activation of the Smad/RUNX2 axis and the overexpression of several AAA progression-related molecules *in vitro*. Compared to their littermates, miR-322 KO mice were susceptible to AngII-induced AAA, whereas the silencing of RUNX2 and the administration of exogenous miR-322 mimics ameliorated the AngII-induced AAA in ApoE KO mice. Overall, we established the roles of the Smad/RUNX2/miR-424/322 axis in AAA pathogenesis. We demonstrated the therapeutic potentials of miR-424/322 mimics and RUNX2 inhibitor for AAA progression.

INTRODUCTION

Rupture of abdominal aortic aneurysm (AAA) is one of the leading causes of sudden death in the elderly population.[1] The mortality rate associated with ruptured AAA can reach 65.9%.[2] Several cardiovascular risk factors, including hypertension, tobacco use, and hyperlipidemia, are associated with the development of both AAA and aortic calcification (AC).[3] Mechanistically, AAA is caused by segmental weakening of the aortic wall and progressive aortic dilation, leading to the eventual rupture of the aorta, accompanied by intense inflammation. Microcalcification and degeneration of the elastic lamina are common pathological features of AAAs.[4,5] An increased degree of calcification has been found in patients with symptomatic or even ruptured AAA compared with those with electively repaired AAA.[6] Intimal calcification disruption is one of the signs of instability for AAA.[7] AC increases aneurysmal wall stress and decreases the biomechanical stability of AAA.[8] AC is also correlated with the location of intimal tears in patients with acute aortic dissection.[9] Vascular smooth muscle cells (VSMCs) synthesize many osteogenic factors during the development of vascular calcification.[10] The overexpression of the Runt-related gene (RUNX) has been found in aneurysmal tissues.[11] The osteogenic transcription factor RUNX2 encodes multifunctional mediators of intracellular signal transduction pathways that affect vascular remodeling and inflammation.[12] RUNX2 is also functionally linked to the regulation of matrix metalloproteinases (MMPs) and angiogenic factors.[12] Angiotensin II (AngII) causes rapid Smad2/3 phosphorylation and nuclear translocation of p-Smad2/3 via TGF-β-independent MAPK activation.[13,14] The activation of Smad-RUNX2 signaling pathway promotes osteogenic differentiation.[15] MicroRNAs (miRNAs) are endogenous RNA fragments that post-transcriptionally repress the expression of target genes, usually by binding to the 3′ untranslated regions (UTRs) of mRNAs. Recent studies have indicated that miRNAs are actively involved in the pathogenesis of AAA through the modulation of inflammatory pathways, endothelial dysfunction, apoptosis of VSMCs and vascular remodeling.[16] Emerging evidence has demonstrated the crucial roles of miR-424/322 (miR-322 is the murine analog of miR-424) in several cardiovascular and respiratory

Received 19 February 2021; accepted 17 December 2021;
https://doi.org/10.1016/j.omtn.2021.12.028.

Correspondence: Shih-Hung Tsai, Department of Emergency Medicine, Tri-Service General Hospital, National Defense Medical Center, No. 325, Section 2, Cheng-Kung Road, Neihu District, Taipei City 11490, Taiwan.
E-mail: tsaishihung@yahoo.com.tw

diseases.[17] miR-424/322 is also recognized as an "osteomir" that modulates calcification.[18] Given the potential role of AC as a relatively late process in the stiffening of the abdominal aorta and its association with AAA progression, reversing calcification could have therapeutic potential in AAAs.[19] Thus, we aimed to evaluate the roles of osteogenic RUNX2 and downstream miR-424/322 in AAA development by determining whether they modulate AAA-related molecules, such as MMPs and vascular endothelial growth factor (VEGF). We further test whether RUNX2 inhibitors and miR-424/322 mimics can mitigate experimental AAA.

RESULTS

Several risk factors for aneurysm induce MMP expression through RUNX2 activation in human aortic smooth muscle cells (HASMCs)

Poorly controlled hypertension and hyperlipidemia and a high prevalence of smoking are associated with persistent AAA-related mortality.[20] Previous studies have indicated that the continuous delivery of AngII and nicotine can induce AAA formation in hyperlipidemic mice.[21] We examined the effects of those representative aneurysm risk factors (i.e., AngII, oxidized PAPC [OxPAPC, a biological active oxidized phospholipid used to mimic proinflammatory effects induced by oxidized lipoproteins], and nicotine)[22–26] on the expression of AAA-related molecules *in vitro*. As shown in Figure 1A, the treatment of HASMCs with aneurysmal prone factors in clinically relevant concentrations (i.e., AngII [1 μM], OxPAPC [10 μg/mL], or nicotine [10 μM]) for 24 h resulted in increased Smad2/3 phosphorylation and RUNX2, MMP-2, MMP-9, and VEGF expression in SMCs. The MMP-2/9 activities are shown in Figure S1. The time dependence of the changes in Smad2/3 phosphorylation and RUNX2 expression and expression of the downstream factors VEGF, MMP-2, and MMP-9 in HASMCs treated with AngII (1 μM) is shown in Figure 1B. To confirm that the AngII-induced increase in MMP and VEGF expression are involved in the RUNX2 and Smad2/3 signaling pathways, we transfected HASMCs with Smad2/3 siRNA (10 nM) and control small interfering RNA (siRNA) (10 nM) before AngII treatment. As shown in Figure 1C, silencing of Smad2/3 effectively reduced Smad2/3 protein expression and attenuated AngII-induced RUNX2, MMP-2, MMP-9, and VEGF expression in HASMCs. This result indicates that RUNX2 is regulated by the Smad2/3 pathway. Furthermore, we found that silencing of RUNX2 reduced RUNX2 protein expression and attenuated AngII-induced VEGF, MMP-2, and MMP-9 expression *in vitro* (Figures 2A and 2B). Through chromatin immunoprecipitation (ChIP) assays and quantitative real-time -PCR, we found that AngII activated the osteoblast-specific elements (OSEs) of VEGF, MMP-2, and MMP-9 via transactivation of RUNX2 (Figure 2C). The primer sequences for MMP-2/9 and VEGF predicted by JASPAR are shown in the supplemental information. To confirm the results of the ChIP assays, we constructed pNL-MMP2, pNL-MMP9, and pNL-VEGF nano luciferase reporter plasmids that included the OSE promoter region and co-transfected HEK 293 cells with these plasmids together with plasmid cytomegalovirus (pCMV)-RUNX2 or the pCMV control plasmid. As shown in Figure 2D, in the MMP-2, MMP-9, and VEGF groups, the luciferase activities were significantly increased 1.8-, 1.2-, and 1.3-fold, respectively, by RUNX2 overexpression compared with control. The data indicate that RUNX2 can bind to the OSE promoter region of MMP2/9 and VEGF.

Silencing of RUNX2 ameliorates AngII-induced AAA *in vivo*

To evaluate the possible effect of RUNX2 on aneurysm formation *in vivo*, we induced AAA in male apolipoprotein E knockout (ApoE KO) mice by continuous infusion of AngII via an osmotic minipump. Male sex is the largest nonmodifiable risk factor for AAA; the incidence of AAA in men is estimated to be 4-5-fold higher than it is in women, and men have a 10-fold higher risk than age-matched women of developing an AAA.[27] Consistent with previous studies, continuous infusion of AngII in the ApoE KO mice induced AAA development in the suprarenal aorta, as shown in Figure 3. These mice were treated with either control siRNA or siRUNX2 (0.2 mg/kg/week). The administration of siRUNX2 significantly reduced the incidence of AngII-induced AAA formation by 40% (Figure 3B), the external aortic diameter by 28% (Figure 3C), and the elastin degradation grade by 53% (Figure 3D). As depicted in Figure 3E, siRUNX2 attenuated the continuous AngII infusion-induced upregulation of MMP-2, MMP-9, and VEGF in homogenates of the aorta. Neovascularization and infiltrates of macrophage and leukocytes are involved in the development of AAA.[28] We found that silencing RUNX2 also attenuated AngII-induced neovascularization (CD31); leukocytes (CD45, leukocyte common antigen), and macrophage (CD68, macrophage) infiltration and microcalcification in the aortas (Figures S2 and S3). In addition, RUNX2 mRNA and protein expression levels were decreased after siRUNX2 treatment (Figures 3E and 3F). The administration of siRUNX2 did not alter systolic blood pressure, serum cholesterol, or body weight (defined as 10% body weight loss). We searched the GEO database of the National Center for Biotechnology Information using the key words "abdominal aortic aneurysm" and "RUNX2." The results revealed that patients with AAA had higher RUNX2 mRNA ($\log^2$) expression than control patients (Figure 3H). Although there were no statistically significant differences in miR-424 expression between control and AAA patients, the AAA patients showed a rising trend (Figure 3I).[29] These findings are consistent with our hypothesis that RUNX2 has a pathogenic role in AAA.

miR-424 mimics reduce AngII-induced protein overexpression in HASMCs *in vitro*

As confirmation of the association between miR-424 and AngII-induced activation of the Smad2/3/RUNX2 axis, using JASPAR online software prediction, we found that several predicted OSE sites in the promoter region of miR-424 could be transactivated (Table S5). Using ChIP and luciferase assays, we evaluated whether RUNX2 transactivates miR-424 promoters. As shown in Figure 4A, quantitative real-time-PCR revealed that OSE expression associated with miR-424 was increased ~5.8-fold in AngII-induced HASMCs in comparison with the control. At the same time, we observed a higher level of luciferase activity in HASMCs co-transfected with pCMV-RUNX2 plasmid and pNL-miR-424 plasmid that included

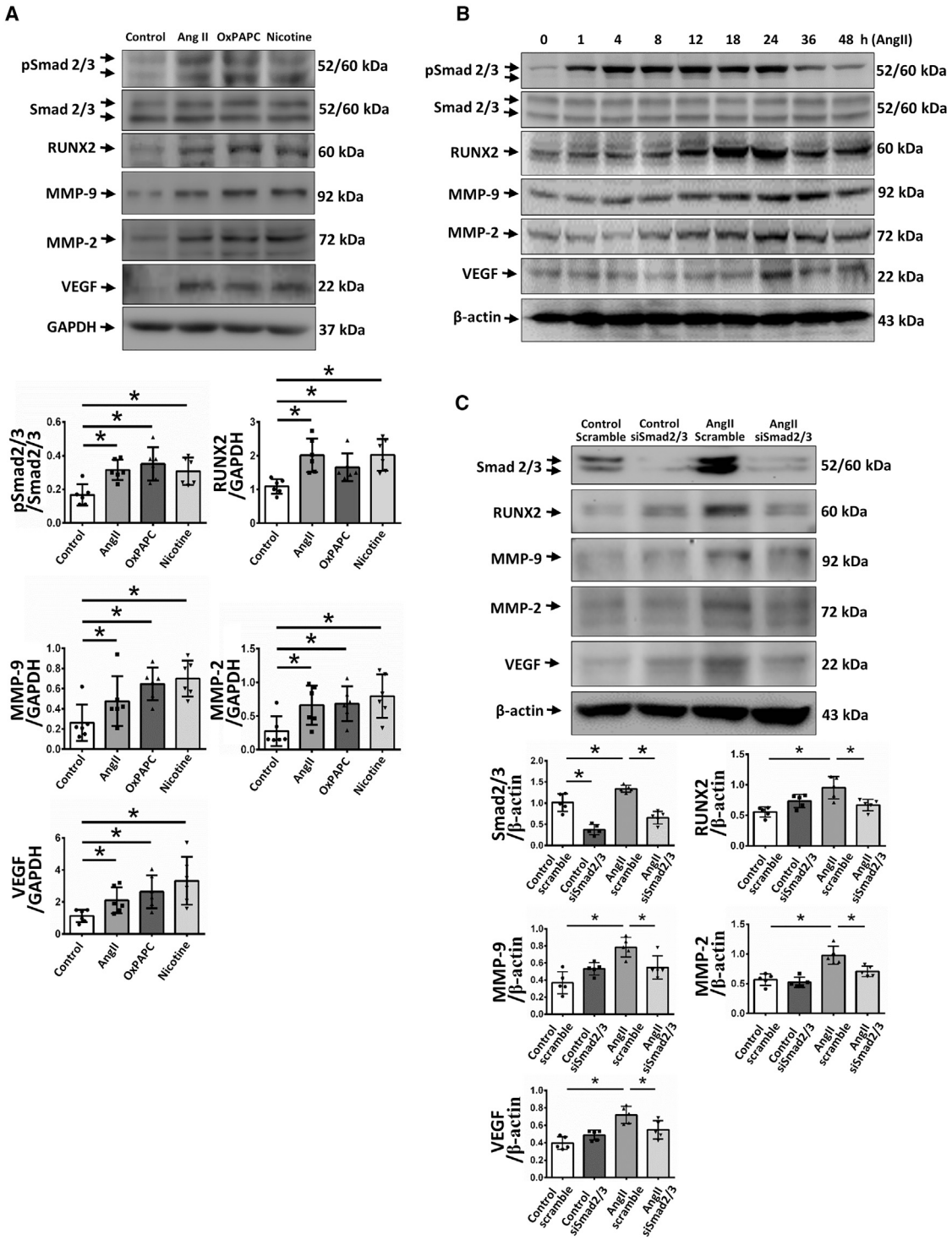

Figure 1. AngII treatment upregulates RUNX2 expression in HASMCs through Smad 2/3 activation

(A) Protein expression in response to 24-h stimulation with agents that increase the risk of aneurysm (AngII, 1 μM; OxPAPC, 10 μg/mL; nicotine, 10 μM); n = 6. (B) Protein expression in response to stimulation with AngII (1 μM) as a function of time. Stripping was performed in Smad2/3 and β-actin. (C) Smad2/3, RUNX2, MMP-2, MMP-9, and VEGF protein expression after AngII treatment with or without Smad2/3 siRNA transfection (n = 5). The data are presented as the mean ± SEM. Statistical significance was determined using 1-way ANOVA followed by a Fisher's least significant difference test (A) and Tukey test (C), *$p < 0.05$.

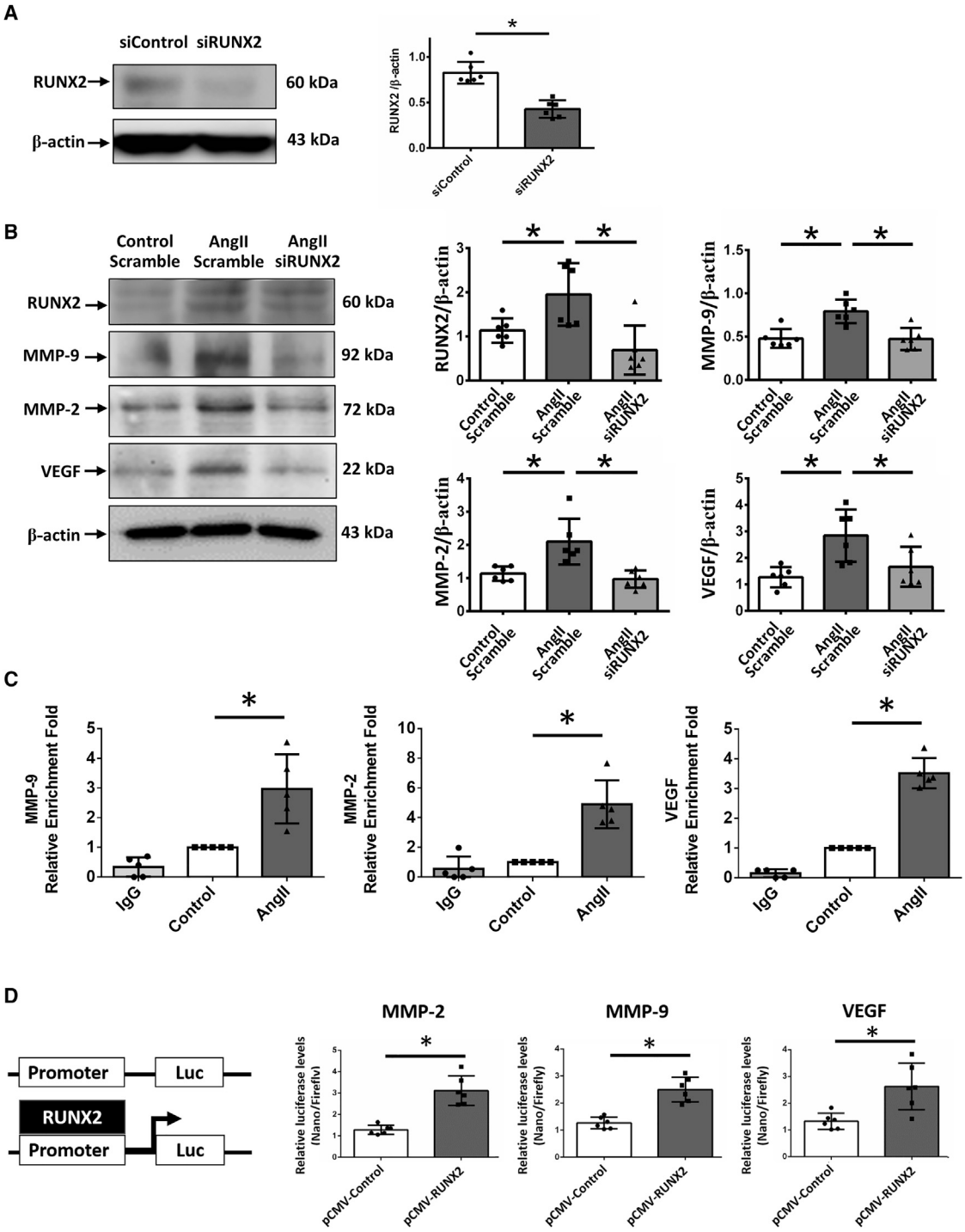

Figure 2. RUNX2 directly induces MMP-2/9 and VEGF expression in AngII-stimulated HASMCs

(A) RUNX2 silencing RNA effectively reduced RUNX2 protein expression (n = 6). (B) Protein expression after AngII treatment (24 h) and transfection with control siRNA (20 nM) or siRUNX2 (20 nM) (n = 6). (C) Promoter activation of MMP-2/9 and VEGF after AngII-induction in HASMCs shown by ChIP assays with rabbit IgG and RUNX2 antibody using quantitative real-time-PCR analysis (n = 5). (D) Promoter activation of MMP-2/9 and VEGF in RUNX2-overexpressing HEK 293 cells using a luciferase assay (n = 6). The data are presented as the mean ± SEM. Statistical significance was determined using 1-way ANOVA followed by a Tukey's test (B and C) or Student t test (A and D). *p < 0.05

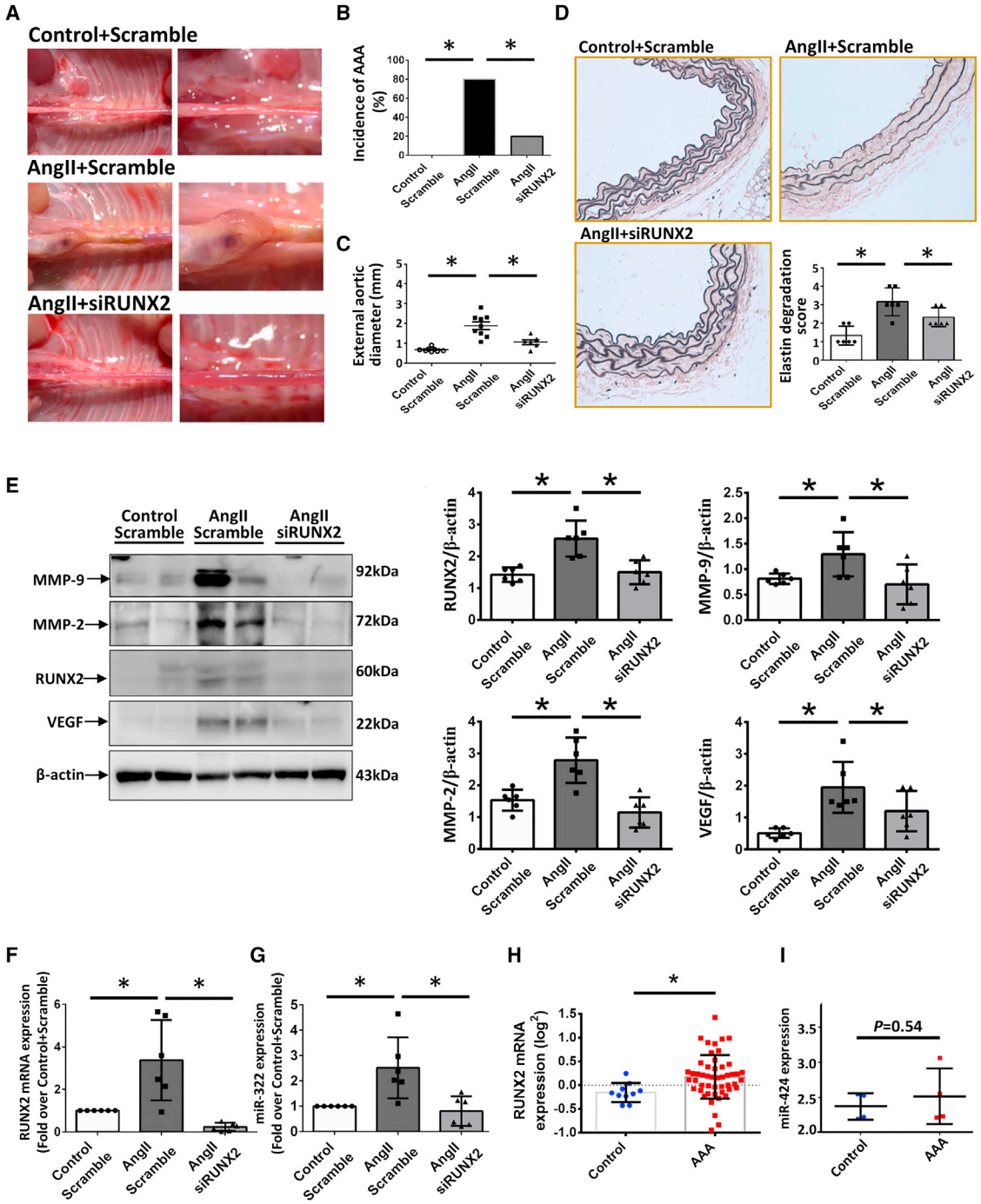

Figure 3. Silencing of RUNX2 attenuates AngII-induced AAA in ApoE-deficient mice *in vivo*

ApoE KO mice that were implanted with AngII (1,000 ng/kg/min)-loaded minipump were treated with either control siRNA or siRUNX2 (0.2 mg/kg/week) via retro-orbital injection. (A) Representative images of the aortas. (B) Incidence of AAA and (C) external diameter of the aortas (n ≥ 6). (D) Elastin degradation grading of the aortas (n = 6). (E) Protein expression in the homogenates of the aortas (n = 6). (F) RUNX2 mRNA expression in the homogenates of the aortas shown by RT-qPCR (n = 6). (G) miR-322 expression in the homogenates of the aortas shown by quantitative real-time-PCR (n = 6). (H) Results of a search of the GEO database for RUNX2: control, n = 10; patients, n = 49. (I) Results of a search of the GEO database for miR-424: control, n = 4; patients, n = 4. The data are presented as the mean ± SEM. Statistical significance was determined using 1-way ANOVA followed by a Tukey's test (A–G) or Student's t test (H and I). *p < 0.05.

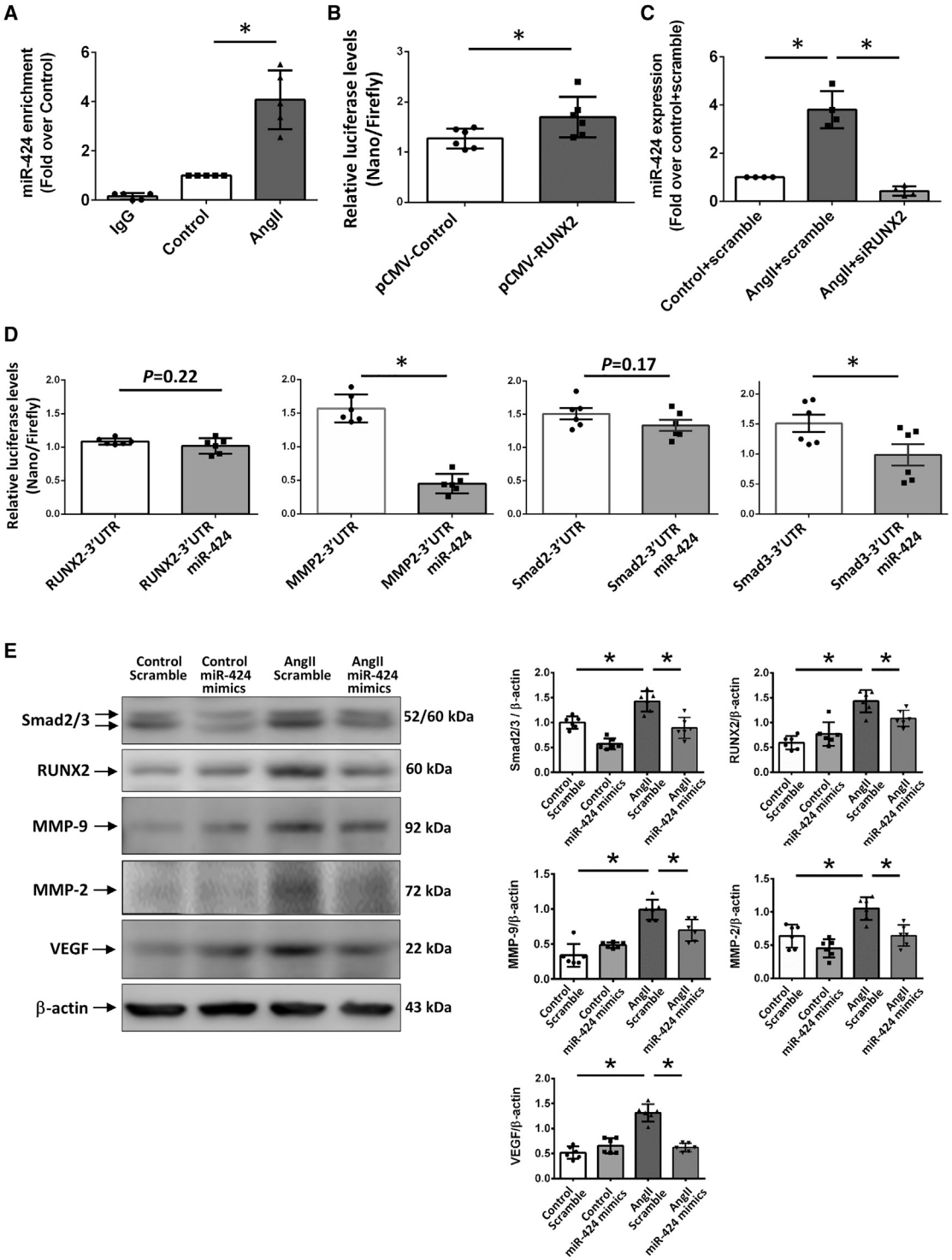

Figure 4. miR-424 is transactivated through AngII-induced RUNX2 and regulates several downstream targets of RUNX2 *in vitro*

(A) Quantitative real-time-PCR results following a ChIP assay with rabbit IgG and RUNX2 antibody showing OSE expression associated with miR-424 expression after AngII treatment (n = 5). (B) Promoter activation of miR-424 in RUNX2-overexpressing HEK 293 cells using a luciferase assay (n = 6). (C) miR-424 expression under AngII stimulation with or without siRUNX2 determined by quantitative real-time-PCR (n = 4). (D) Dual-luciferase level showing binding of miR-424 and the 3′UTR of target genes determined by a luciferase assay in HEK 293 cells (n = 6). (E) Protein expression after miR-424 mimic transfection in AngII-induced HASMC (n = 6). The data are presented as the mean ± SEM. Statistical significance was determined using Student's t test (B and D) or 1-way ANOVA followed by a Tukey's test (A, C, and E). *p < 0.05.

the OSE promoter region; the luciferase activity of the co-transfected cells showed an ~1.8-fold increase in comparison with HASMCs co-transfected with the pCMV-control plasmid (Figure 4B). To further confirm that miR-424 could be modulated by RUNX2, we used RNA interference to knock down RUNX2 expression in HASMCs subjected to AngII induction. As shown in Figure 4C, silencing RUNX2 resulted in a decrease in miR-424 expression of ~3.3-fold compared with AngII treatment. Furthermore, to investigate the role of miR-424 expression in the Smad2/3/RUNX2 axis, we searched the target mRNAs of miR-424 in TargetScan and miRanda online software and found that the 3′ UTRs of Smad2/3, RUNX2, MMP-2, and VEGF could be targeted by miR-424 (Table S6). To validate the predicted targets of miR-424, we cloned the 3′-UTR fragments with target sequences into a pNL luciferase reporter vector. The sequences of the binding sites are shown in Table S6. As shown in Figure 4D, the luciferase activities of the cells transfected with pNL-Smad3 or pNL-MMP-2 were reduced by the overexpression of miR-424. In addition, in our previous study, we found that miR-424 binds to the 3′UTR of VEGF.[30] In summary, these data suggest that Smad3, MMP-2, and VEGF mRNA may be direct targets of miR-424. The administration of miR-424 mimics reduced the AngII-induced activation of Smad2/3 and overexpression of RUNX2, MMP-2, MMP-9, and VEGF in HASMCs *in vitro* (Figures 4E and S4). We did not anticipate that miR424/322 would modulate the phosphorylation or activation Smad2/3 pathway. Our data indicate that miR-424 is part of a negative feedback loop that controls the Smad2/3/RUNX2 axis.

miR-322-deficient mice are susceptible to AngII-induced AAA, and exogenous miR-322 mimics ameliorate AngII-induced AAA

As expected, significantly decreased miR-322 expression levels were observed in the aortas of miR-322 KO mice compared to their littermates (Figure 5A). To evaluate the possible effect of miR-322 on aneurysm formation, we induced AAA by continuous infusion of AngII in miR-322 KO mice. The results indicate that the miR-322 KO mice were more susceptible to AngII infusion-induced aortic expansion than their littermates (Figures 5B and 5C). The AngII-infused miR-322 KO mice had a significantly higher (60% higher) incidence of AAA than their AngII-infused littermates (Figure 5D). In addition, the AngII-infused miR-322 KO mice showed significantly increased elastin degradation (Figure 5E). Increased Smad2/3, RUNX2, MMP9, MMP2, and VEGF protein levels were also observed in the aortas of miR-322 KO mice subjected to AngII infusion (Figure 5F). No significant difference was observed between the two groups with respect to changes in body weight (defined as the loss of 10% of body weight) during the study period. Previous studies have indicated that miR-424/322 regulates osteogenesis,[31,32] and our findings also showed that miR-322 KO mice subjected to AngII infusion exhibited microcalcification in comparison with littermates subjected to AngII infusion (Figure S3).

We further found that exogenous miR-322 mimics significantly reduced the incidence of AAA formation from 80% to 50% (Figure 6B) and attenuated AngII-induced aortic expansion (Figure 6C). As expected, exogenous miR-322 mimics attenuated the AngII-induced elastin degradation score (Figure 6D). Exogenous miR-322 mimics not only increased miR-322 expression but also significantly decreased MMP-2, MMP-9, Smad2/3, VEGF, and RUNX2 protein expression in the aortas of AngII-infused ApoE KO mice (Figure 6F). In addition, miR-322 mimics attenuated AngII-induced CD31, CD45, and CD68 expression in aortas (Figure S2). The body weight changes in the two groups showed no significant differences during the study period. Thus, miR-322 inhibits AAA progression through the regulation of the Smad2/3/RUNX2 axis.

DISCUSSION

In the present study, we demonstrated the crucial roles of the Smad2/3/RUNX2/miR-424/322 axis in AAA progression. Specifically, we found that (1) miR424/322 modulates the Smad2/3/RUNX pathway by inhibiting Smad3, MMP-2, and VEGF; (2) silencing RUNX2 and exogenous miR-322 mimics ameliorate AngII-induced AAA formation in ApoE KO mice; and (3) RUNX2 transcriptionally activates miR-424 expression.

In the Aneurysm Global Epidemiology Study, a positive linear relationship was found among trends in hypertension, cholesterol, and smoking prevalence and AAA growth in patients with AAA.[20] Close correlations have been found between vascular calcification (VC) and degeneration and inflammation of the aorta. The overexpression of RUNX2 has been found in human aneurysmal tissues.[11,33] In animal experiments, exogenous AngII, nicotine, and hyperlipidemia have been shown to induce RUNX2 overexpression and VC. RUNX2 is required for the overexpression of oxidized low-density lipoprotein-induced osteogenic factor.[10] A recent study suggested that RUNX2 mediates microcalcification, further elevation of inflammatory factor levels, and MMP expression in AngII-induced AAA.[4] VSMC-specific RUNX2 deletion inhibited AngII-induced microcalcification and AAA formation in ApoE KO mice.[4] We confirmed that RUNX2 directly promotes AAA formation through the overexpression of VEGF and MMPs.

The role of the transforming growth factor-β (TGF-β) signaling pathway in AAA pathogenesis is still controversial.[21] Previous studies have indicated that TGF-β inhibition augments AngII-induced AAAs, with the majority exhibiting rupture.[34] Dysregulated TGF-β pathways have been shown to be correlated with aortic diameter in humans and in experimental models of aneurysm formation.[35] Recently, AngII was reported to cause rapid Smad2/3 phosphorylation and nuclear translocation of p-Smad2/3 via TGF-β-independent MAPK activation.[13,14] Here, we demonstrated that risk factors for aneurysm induced RUNX2 overexpression through the activation of Smad2/3, suggesting that AAA progression, as well as calcification, are facilitated by the activation of the Smad2/3 pathway.

RUNX2 further promotes AAA formation by transactivating MMP-2, MMP-9, and VEGF. MMP activation participates in the progression of both VC and AAA.[36] MMP-2 and MMP-9 promote VC by upregulating RUNX2 signaling, resulting in VSMC phenotypic

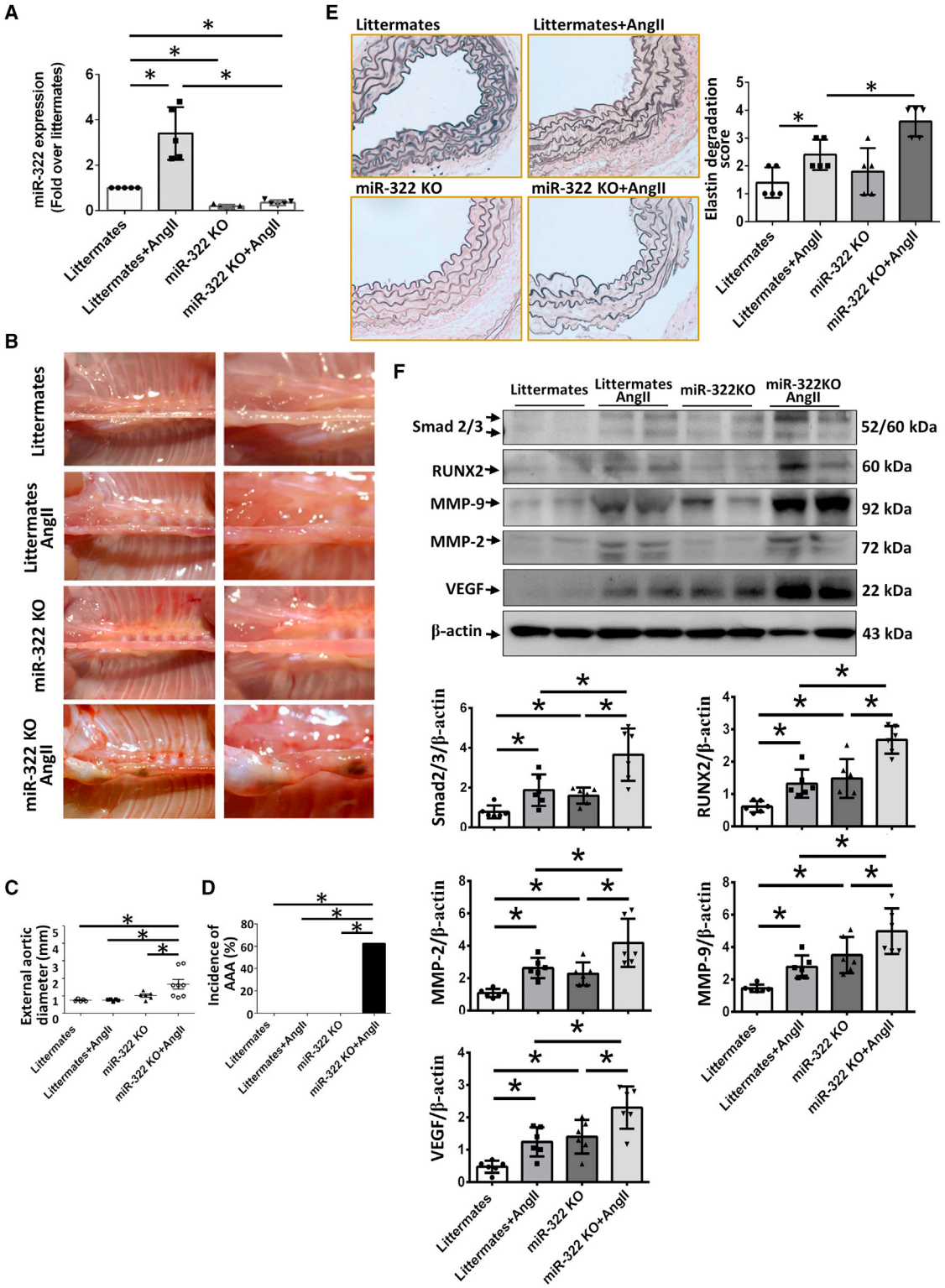

Figure 5. miR-322-deficient mice are susceptible to AngII-induced AAA

Implantation of AngII (1,000 ng/kg/min)-loaded minipumps in miR-322 KO mice and their littermates. (A) miR-322 expression in aorta homogenates (n = 5). (B) Representative images of the aortas. (C) External diameter of the aortas (n ≥ 5). (D) Incidence of AAA and (E) elastin degradation grading of the aortas (n = 5). (F) Protein expression in homogenates of the aortas (n = 6). The data are presented as the mean ± SEM. Statistical significance was determined using 1-way ANOVA followed by a Tukey's test. *$p < 0.05$.

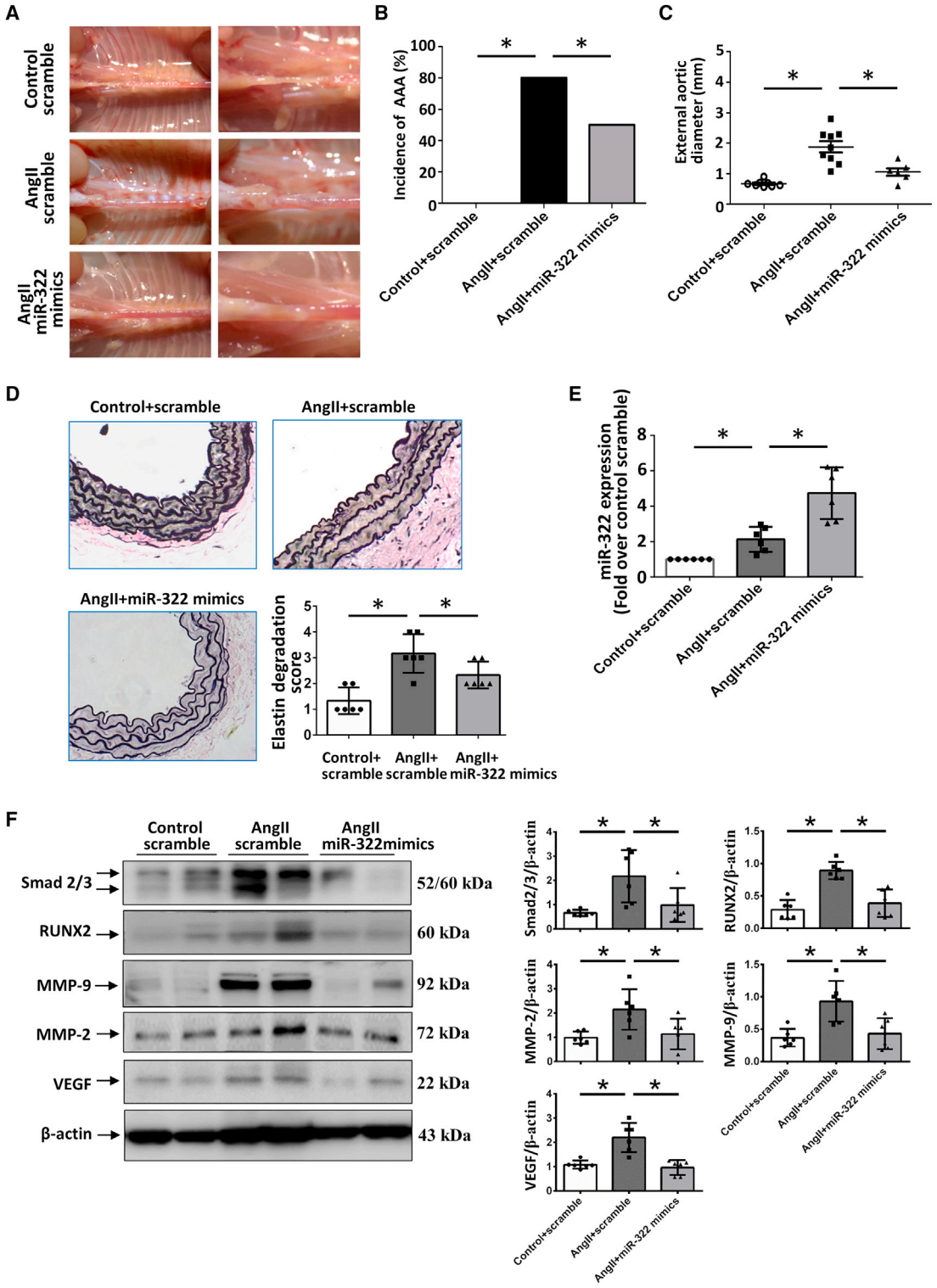

Figure 6. Exogenous miR-322 attenuates AngII-induced AAA in ApoE-deficient mice *in vivo*

ApoE KO mice that were implanted with AngII (1,000 ng/kg/min)-loaded minipumps were treated with either control mimics or miR-322 mimic (2 mg/kg/week) via retro-orbital injection. (A) Representative images of the aortas. (B) Incidence of AAA and (C) external diameter of the aortas (n = 6). (D) Elastin degradation grading of the aortas (n = 6). (E) miR-322 expression in the homogenates of the aortas (n = 6). (F) Protein expression in homogenates of the aortas (n = 6). The data are presented as the mean ± SEM. Statistical significance was determined using 1-way ANOVA followed by a Tukey's test. *$p < 0.05$.

conversion and matrix remodeling.[37] The silencing of RUNX2 has been shown to reduce pulmonary artery remodeling and prevent calcification, thus improving pulmonary hemodynamic parameters and right ventricular function.[38]

Recent advances in molecular biology have led to the identification of several miRNAs and transcription factors that are involved in the process of AAA formation.[39] miRNAs can simultaneously modulate many genes, often regulating individual signaling pathways at multiple levels.[40] We found that Smad3, MMP-2, and VEGF are targets of miR-424/322. Previous studies have indicated that miR-424 modulates bone formation and targets RUNX2 and that the downregulation of miR-424 is associated with the osteodifferentiation of mesenchymal stem cells.[31] Another study found that decreased miR-424 expression facilitated osteogenic differentiation, suggesting that miR-424 inhibits alkaline phosphatase (ALP) activity, calcium deposition, and Smad2/3/RUNX2 axis expression.[32] Several reports have indicated that miR-424/322 is present in endothelial cells, macrophages, and fibroblasts.[30,34,41] We are aware that AAA development is multifactorial in origin and that several vascular cell types may be involved.

Consistent with these observations, our findings indicate that miR-424/322 inhibits the expression of osteogenic markers, including Smad2/3 and RUNX2. miR-424 actively participates in adaptation to hypoxia and prevents acute hypoxia-induced pulmonary vascular leakage by modulating the hypoxia-inducible factor-1 α(HIF-1α)-VEGF axis.[30,42] VEGF contributes to AAA formation by promoting inflammation and neovascularization. VEGF overexpression in vascular cells was found in the aneurysmal wall compared with the normal abdominal aorta.[43] Exogenous VEGF has been found to increase the formation of AngII-induced aneurysms, whereas treatment with soluble VEGF-A receptor inhibited AAA development in mice.[44,45] Recombinant VEGF protein treatment dose dependently increases the transcriptional activity of RUNX2.[46] Through the targeting of Smad3, MMP-2, and VEGF, miR-424/322 exerts protective effects against AAA progression.

No studies have shown that commonly used cardiovascular drugs have clinical benefits with respect to AAA progression.[47] Here, we propose another pathway that offers a potential intervention site for the medical treatment of AAA. Associations between aortic calcification and aortic disease have been found. Most incidental AAAs are below the threshold for intervention at the time of detection. In a recent Swedish study involving ultrasonographic screening of 65-year-old men, the prevalence of abdominal aortic aneurysms was 2.2%, whereas in earlier studies, the reported prevalence was as high as 8% among men 65 to 80 years of age.[48–50] The risk of AAA rupture is determined by the size of the aneurysm; rupture occurs in ∼2% of AAAs <4 cm in diameter and in >25% of AAAs >5 cm. Surgical repair is indicated for large AAAs (diameter >5.5 cm) and when the growth rate of AAAs exceeds 1 cm/year.[51] Therefore, in addition to current cardiovascular risk-reducing treatments, adjunctive medical therapy targeting the regulation of extracellular matrix (ECM) metabolism is still required in clinical settings.[51] Recent advances in molecular biology have led to the identification of several miRNAs and transcription factors that participate in the process of AAA formation. Nucleic acid drugs are expected to be a novel therapeutic option for AAA.[52]

Limitations of the study

We are aware that AAA development is multifactorial in origin and that several vascular cell types may be involved; miR424/322 is also present in endothelial cells and in monocytes/macrophages.[5,30,34,41] In the GEO data, miR-424 expression showed a rising trend in patients with AAA, but the difference between AAA patients and controls was not significant. Therefore, miR-424 expression should be checked in the clinical setting. The roles of RUNX2 and miR-424/322 in other inflammatory cells should be explored further. Whereas global RUNX2 KO can be fatal, tissue-specific RUNX2 and miR-322 KO mice can be used to further elucidate the role of this axis in AAA pathogenesis.

Conclusions

The Smad/RUNX2/miR-424/322 axis is crucial for AAA development. RUNX2 inhibition and miR-322 mimics attenuated experimental AngII-induced AAA formation *in vivo*.

MATERIALS AND METHODS

The data that support the findings of this study are available from the corresponding author on reasonable request.

Gene Expression Omnibus (GEO) database

The National Center for Biotechnology Information (NCBI) GEO database was used to assess the expression of RUNX2 and miR-424 in clinical AAA samples.[53,54] The key word *abdominal aortic aneurysm* was used in the search, and normal control and AAA samples in the same database were identified as screening criteria for further analysis (https://www.ncbi.nlm.nih.gov/geoprofiles/?term=aortic%20aneurysm%2C%20RUNX2). We used microarray databases in the search. For RUNX2 mRNA expression, the Database: GSE57691 database was used. The microarray platform for the Database: GSE57691 database is GPL10558 [ilmn_HumanHT_12_V4_0], and the versions used are R 3.2.3, Biobase 2.30.0, GEOquery 2.40.0, limma 3.26.8. We used an Illumina HumanHT-12 V4.0 expression beadchip in which 10 samples from healthy donors and 49 samples from patients with varying degrees of AAAs were included.[55] Another Database: GSE7084 database was used for miR-424 expression. The microarray platform for the Database: GSE7084 database is GPL570 [HG-U133_Plus_2], an Affymetrix Human Genome U133 Plus 2.0 Array in which 4 samples from healthy male donors (GSM170551, GSM170553, GSM170554, and GSM170555) and 4 samples from male AAA patients (GSM170557, GSM170559, GSM170561, and GSM170562) were included.[29] The RUNX2 mRNA and miR-424 expression profiles were downloaded and extracted using the R GEOquery package (GEOquery 2.40.0, limma 3.26.8) and the R Biobase package (R 3.2.3, Biobase 2.30.0). Informed written consent was deemed not necessary since the data were extracted from the publicly accessible anonymous GEO database.

Cell cultures and reagents

HASMCs were purchased from ScienCell Research Laboratories (#6110, Carlsbad, CA, USA) and maintained in M231 medium (#M231500) with supplemental medium (#S00725) and 5% fetal bovine serum (#10437028). The cells were incubated at 37°C in a 5% CO_2 atmosphere. AngII (Sigma, A9525), nicotine (Sigma, N3876), and oxidized 1-palmitoyl-2-arachidonyl-*sn*-glycerol-3-phosphocholine (OxPAPC, InvivoGen, # tlrl-oxp1) were purchased from Sigma-Aldrich and InvivoGen. siRNA-targeting RUNX2 (siRUNX2) and scrambled RNA were used in the *in vitro* and *in vivo* experiments. miR-322 mimics, interfering RNA, and all culture media were purchased from Life Technologies (Carlsbad, CA, USA).

Generation of miR-322 KO mice

miR-322 KO mice were established on a C57BL/6J background using CRISPR-Cas9 genomic editing, as previously described.[30] Homozygous miR-322 KO mice were obtained; they and their wild-type (WT) littermates were used as the experimental and control groups, respectively.

AngII-induced AAA model

Male ApoE KO mice and male miR-322 KO mice on a C57BL/6J background were maintained on a 12 h/12 h light/dark cycle. ApoE KO mice were obtained from The Jackson Laboratory. During the AAA experiment, the mice were fed a high-fat diet (TestDiet, 58Y1) with food available *ad libitum*. Alzet osmotic minipumps (model 2004; Alzet Scientific Products, Mountain View, CA, USA) were implanted into the mice at 8–10 weeks of age. The pumps were filled with solutions of AngII (Sigma Chemical, St. Louis, MO, USA) and delivered 1,000 ng/kg/min AngII for 28 days, as previously described.[56] The pumps were placed into the subcutaneous space in mice that had been anesthetized with Zoletil 50 (10 mg/kg)/xylazine (0.1 mg/kg, given intraperitoneally) through a small incision in the back, which was then closed with surgical clips. The mice were considered adequately anesthetized when they made no attempt to withdraw a limb after pressure was applied. At the end of the study, the mice were euthanized by exsanguination under anesthesia. Blood was withdrawn from the right ventricle for analysis. After careful removal of the periaortic soft tissue, the entire aorta was perfused with saline and excised. The aorta was then subjected to formalin fixation and paraffin embedding or freezing at −80°C. The body weight of the animals was monitored during treatment to assess side effects. All of the experimental protocols and procedures were approved by the Institutional Animal Care Committee of the National Defense Medical Center (Taipei, Taiwan) and complied with the *Guide for the Care and Use of Laboratory Animals* published by the US National Institutes of Health (eighth edition, 2011).[57]

Delivery of siRNA-targeting RUNX2 and miR-322 *in vivo*

For AAA studies that used silencing by siRUNX2 and miR-322 mimics, mice were injected with RUNX2 siRNA (siRUNX2, 0.2 mg/kg/week for 4 weeks, Life Technologies, #4457298), LNA miR-322 mimics (2 mg/kg/week for 4 weeks, Life Technologies, #4464070) or control siRNA (Life Technologies, #4464058) and control mimics (Life Technologies, #4464061). siRUNX2 or miR-322 mimics were complexed with a transfection reagent (Invivofectamine 3.0, IVF3005, Life Technologies) according to the manufacturer's guidelines to achieve the adequate suppression of target genes. Specifically, solutions of siRUNX2 or miR-322 mimics in complexation buffer were mixed with Invivofectamine 3.0 reagent, and the mixture was incubated at 50°C for 30 min to allow the formation of complexes. The mixture was then injected into the mice retro-orbitally under adequate anesthesia.

Determination of blood pressure and serum lipid profiles

Systolic blood pressure was determined in conscious mice using a tail-cuff apparatus (Softron BP-98A tail blood pressure system, Tokyo, Japan). Before the formal measurement, the mice were acclimated to the device on 2 consecutive days. The first 10 blood pressure measurements were discarded. The values obtained in the following 5 consecutive measurements were recorded and averaged. Serum was obtained by centrifugation of blood at 3,000 rpm for 10 min at room temperature. Serum high-density lipoprotein (HDL) cholesterol and low-density lipoprotein (LDL) cholesterol were determined using a Siemens Dimension EXL chemistry analyzer (Siemens, Munich, Germany).

Characteristics and quantification of AAA

After perfusion fixation with cold 4% paraformaldehyde (Sigma, 441,244), the aorta was exposed under a dissecting microscope, and the periadventitial tissue was removed from the aortic wall. The gross appearance of the aorta was recorded via digital photography, and the maximal external diameter of the suprarenal aorta was measured using imaging processing software (ImageJ, National Institutes of Health). Outgrowth of >50% indicated the development of aortic aneurysm, as previously described.[58]

Histology and immunohistochemistry

The harvested aortic tissues were fixed in cold 4% paraformaldehyde for 48 h and stored in 70% ethanol for 12 h. The fixed aortas were embedded, cut in cross-section (5 μm), and stained with hematoxylin and eosin and Verhoeff-Van Gieson (VVG; Sigma, HT25A) for elastin. The severity of elastin degradation was scored semiquantitatively, as previously described (grade 1, no degradation; grade 2, mild degradation; grade 3, severe degradation; and grade 4, presence of aortic rupture).[59]

Immunoblotting

To prepare cell protein lysates, HSAMCs were collected and lysed in protein extraction buffer (E153A, Promega, Madison, WI, USA) containing protease and phosphatase inhibitors (Roche #04693159001 and #04906837001, Roche, Basel, Switzerland). The supernatants obtained by centrifugation of the lysates at 12,000 × *g* for 15 min at 4°C were used in western blotting. To prepare tissue protein lysates, aorta tissue in protein extraction buffer supplemented with protease and phosphatase inhibitors was homogenized using a homogenizer (FastPrep-24 5G, MP Biomedicals, Santa Ana, CA, USA) and centrifuged at 12,000 × *g* for 15 min at 4°C. The supernatants were

collected and subjected to SDS-PAGE followed by electroblotting onto a polyvinylidene fluoride (PVDF) membrane (IPVH00010a, Millipore, Burlington, MA, USA). The membranes were probed with monoclonal antibodies against RUNX2 (#8486, Cell Signaling Technology, Danvers, MA, USA), VEGF (#555036, BD Biosciences, Franklin Lakes, NJ, USA), MMP-2 (GTX104577, GeneTex, Irvine, CA, USA), MMP-9 (GTX100458, GeneTex) and phospho-Smad2/3 (#8828, Cell Signaling Technology). The membranes were incubated with stripping buffer (#786-119, Geno Technology, St. Louis, MO, USA) for 10 min at room temperature and washed with PBS 0.1% Tween (PBST) 3 times for 5 min each in washing buffer, per the manufacturer's recommendation. After re-blocking for 1 h, Smad2/3 (#8685, CST) and β-actin (#MAB1501, Millipore) were used. Bands were visualized using chemiluminescence detection reagents (WBKLS0500, Millipore). Densitometric analysis was conducted with imaging processing software (Multi Gauge, Fujifilm, Tokyo, Japan). Target protein expression measured by immunoblotting was determined via densitometry and is expressed relative to an internal control or as phosphorylated protein relative to total protein expression.

ChIP assay

ChIP assays were performed as previously described.[30] In brief, confluent cells were crosslinked with 4% paraformaldehyde (Sigma, 441,244), and the crosslinking was stopped by the addition of glycerin (Sigma, G8898). The cells were then washed with cold PBS and lysed in FA lysis buffer. Sheared chromatin was subjected to immunoprecipitation with a RUNX2 antibody (#8486, Cell Signaling Technology) or immunoglobulin G (IgG; #2729, Cell Signaling Technology) followed by purification using Protein A/G Dynabeads (GE17152104010150, Merck, Kenilworth, NJ, USA). Protein and RNA were then degraded using Proteinase K (100 μg) and RNase A (1 μg), respectively. The purified chromatin DNA was subjected to quantitative real-time-PCR. The data are expressed as fold change relative to IgG with RUNX2 antibody.

Primer sequences used in ChIP assays

To predict the potential RUNX2 DNA-binding elements, called OSEs, on miR-424, MMP-2, MMP-9, and VEGF, we analyzed selected human and mouse genes using the position weight matrix algorithm from JASPAR (http://jaspar.genereg.net/) to scan the promoter regions of each gene. The promoter region was defined as the region −5,000 to 0 nucleotides from the transcription start site. The sequences of the primers used to detect RUNX2 binding to several potential RUNX2 binding sites in the human miR-424, MMP-2, MMP-9, and VEGF promoter regions are shown in the supplemental information.

Dual-luciferase reporter assay

To confirm that miR-424 binds to the predicted target mRNAs, the 3′UTRs of the target mRNAs were subcloned into a pNL (Nluc) vector (#N1001, Promega). HEK 293 cells were cultured in 6-well plates and co-transfected with 0.5 μg pNL plasmid and 50 μM miR-424 mimics using Lipofectamine 2000 (11,668, Invitrogen, Waltham, MA, USA). To confirm the results of the ChIP assays, we constructed pNL-MMP2, pNL-MMP9, and pNL-VEGF nano luciferase reporter plasmids that included the OSE promoter region and co-transfected HEK 293 cells with these plasmids together with pCMV-RUNX2 or the pCMV control plasmid. The OSE sequences in miR-424, MMP-2, MMP-9, and VEGF promoter regions are shown in the supplemental information. After incubation for 24 h, the cells were lysed, and the nano luciferase activity was measured with a luminometer using a dual-luciferase reporter assay system (#1610, Promega). The ratio of nano luciferase activity to firefly luciferase activity was calculated.

Quantitative real-time-PCR

miRNA was extracted using TRIzol reagent (15596018, Ambion, Austin, TX, USA). cDNA was prepared using a Taqman miRNA Reverse Transcription Kit (#4366596, Life Technologies). Primers for miR-424 and miR-322 were prepared using a Taqman miRNA assay (#4427975 and #4427975, Life Technologies). Quantitative real-time-PCR was performed with Taqman and a QuantStudio 3 Real-Time PCR System (Life Technologies) according to the manufacturer's instructions. The results obtained by quantitative analysis of the quantitative real-time-PCR data for target genes and miR-424/miR-322 are expressed as fold change relative to internal controls or U6 expression.

Zymography

Gelatin zymography was used to determine the gelatinolytic activities of MMP-2 and MMP-9 in aorta homogenates and in conditioned medium, as previously described. Briefly, equivalent amounts of sample were electrophoresed under non-reducing conditions in 7.5% SDS-PAGE containing 0.1 mg/mL gelatin as substrate. The gels were washed in a buffer containing 2.5% Triton X-100 for 1 h to remove SDS and then incubated with a substrate buffer at 37°C for 18 h. MMP activities were quantified by densitometry scanning. Densitometric analysis was conducted with imaging processing software (Multi Gauge, Fujifilm).

Statistical analysis

All of the experiments were performed independently at least 3 times, and all of the continuous variables are presented as the mean ± standard error of the mean (SEM). The F test for equal variance was performed before the differences among groups were analyzed. Comparisons between two groups were analyzed using Student's t test. For multiple groups, the data were analyzed using one-way ANOVA. For post hoc analysis, a Tukey test was applied to correct for multiple comparisons, and a Fisher's least significant difference test was used for planned comparisons. Statistical significance was defined as $p < 0.05$. Analyses were performed using a statistical software package (SPSS version 16.0 for Windows; SPSS, Chicago, IL, USA).

SUPPLEMENTAL INFORMATION

Supplemental information can be found online at https://doi.org/10.1016/j.omtn.2021.12.028.

ACKNOWLEDGMENTS

This study was supported by a grant from Tri-Service General Hospital, National Defense Medical Center, Taipei, Taiwan (TSGH-C108-067, TSGH-D-109071, and TSGH-E-110222) and by the Ministry of National Defense-Medical Affairs Bureau (MAB-108-018, MAB-109-035, MAB-110-121), Cheng Hsin General Hospital-National Defense Medical Center (CH-NDMC108-30, CHNDMC-109-16 and CHNDMC-110-106) and the Ministry of Science and Technology, Taiwan (MOST 107-2314-B-016-061 and MOST 108-2314-B-016-047-MY3).

AUTHOR CONTRIBUTIONS

Y.-J.H. and S.-H.T. conceptualized the study. H.-Y.T., J.-C.W., C.-Y.L., and Y.-L.C. collated and curated the data. Y.-L.C. performed the formal analysis. J.-C.W. and S.-H.T. acquired the funding. C.-Y.L., H.-Y.T., and S.-H.T. performed the methodology. Y.-J.H. provided the resources. H.-Y.T. and S.-H.T. wrote the original draft. All of the authors have read and approved the final submitted manuscript.

DECLARATION OF INTERESTS

The authors declare no competing interests.

REFERENCES

1. Hirsch, A.T., Haskal, Z.J., Hertzer, N.R., Bakal, C.W., Creager, M.A., Halperin, J.L., Hiratzka, L.F., Murphy, W.R., Olin, J.W., Puschett, J.B., et al. (2006). ACC/AHA 2005 practice guidelines for the management of patients with peripheral arterial disease (lower extremity, renal, mesenteric, and abdominal aortic): a collaborative report from the American association for vascular surgery/society for vascular surgery, society for cardiovascular angiography and interventions, society for vascular medicine and biology, society of interventional radiology, and the ACC/AHA task force on practice guidelines (writing committee to develop guidelines for the management of patients with peripheral arterial disease): endorsed by the American association of cardiovascular and pulmonary rehabilitation; national heart, lung, and blood institute; society for vascular nursing; TransAtlantic inter-society consensus; and vascular disease foundation. Circulation *113*, e463–e654.

2. Karthikesalingam, A., Holt, P.J., Vidal-Diez, A., Ozdemir, B.A., Poloniecki, J.D., Hinchliffe, R.J., and Thompson, M.M. (2014). Mortality from ruptured abdominal aortic aneurysms: clinical lessons from a comparison of outcomes in England and the USA. Lancet *383*, 963–969.

3. Youssef, G., Guo, M., McClelland, R.L., Shavelle, D.M., Nasir, K., Rivera, J., Carr, J.J., Wong, N.D., and Budoff, M.J. (2015). Risk factors for the development and progression of thoracic aorta calcification: the multi-ethnic study of atherosclerosis. Acad. Radiol. *22*, 1536–1545.

4. Li, Z., Zhao, Z., Cai, Z., Sun, Y., Li, L., Yao, F., Yang, L., Zhou, Y., Zhu, H., Fu, Y., et al. (2020). Runx2 (runt-related transcription factor 2)-mediated microcalcification is a novel pathological characteristic and potential mediator of abdominal aortic aneurysm. Arterioscler. Thromb. Vasc. Biol. *40*, 1352–1369.

5. Quintana, R.A., and Taylor, W.R. (2019). Cellular mechanisms of aortic aneurysm formation. Circ. Res. *124*, 607–618.

6. Buijs, R.V., Willems, T.P., Tio, R.A., Boersma, H.H., Tielliu, I.F., Slart, R.H., and Zeebregts, C.J. (2013). Calcification as a risk factor for rupture of abdominal aortic aneurysm. Eur. J. Vasc. Endovasc. Surg. *46*, 542–548.

7. Sever, A., and Rheinboldt, M. (2016). Unstable abdominal aortic aneurysms: a review of MDCT imaging features. Emerg. Radiol. *23*, 187–196.

8. Li, Z.Y., U-King-Im, J., Tang, T.Y., Soh, E., See, T.C., and Gillard, J.H. (2008). Impact of calcification and intraluminal thrombus on the computed wall stresses of abdominal aortic aneurysm. J. Vasc. Surg. *47*, 928–935.

9. Yang, C.J., Tsai, S.H., Wang, J.C., Chang, W.C., Lin, C.Y., Tang, Z.C., and Hsu, H.H. (2019). Association between acute aortic dissection and the distribution of aortic calcification. PLoS One *14*, e0219461.

10. Farrokhi, E., Samani, K.G., and Chaleshtori, M.H. (2015). Oxidized low-density lipoprotein increases bone sialoprotein expression in vascular smooth muscle cells via runt-related transcription factor 2. Am. J. Med. Sci. *349*, 240–243.

11. Dubis, J., Litwin, M., Michalowska, D., Zuk, N., Szczepanska-Buda, A., Grendziak, R., Baczynska, D., Barc, P., and Witkiewicz, W. (2016). Elevated expression of runt-related transcription factors in human abdominal aortic aneurysm. J. Biol. Regul. Homeost. Agents *30*, 497–504.

12. Niu, D.F., Kondo, T., Nakazawa, T., Oishi, N., Kawasaki, T., Mochizuki, K., Yamane, T., and Katoh, R. (2012). Transcription factor Runx2 is a regulator of epithelial-mesenchymal transition and invasion in thyroid carcinomas. Lab. Invest. *92*, 1181–1190.

13. Rodríguez-Vita, J., Sánchez-López, E., Esteban, V., Rupérez, M., Egido, J., and Ruiz-Ortega, M. (2005). Angiotensin II activates the Smad pathway in vascular smooth muscle cells by a transforming growth factor-beta-independent mechanism. Circulation *111*, 2509–2517.

14. Wang, W., Huang, X.R., Canlas, E., Oka, K., Truong, L.D., Deng, C., Bhowmick, N.A., Ju, W., Bottinger, E.P., and Lan, H.Y. (2006). Essential role of Smad3 in angiotensin II-induced vascular fibrosis. Circ. Res. *98*, 1032–1039.

15. Wang, H., Chen, F., Li, J., Wang, Y., Jiang, C., Wang, Y., Zhang, M., and Xu, J. (2020). Vaspin antagonizes high fat-induced bone loss in rats and promotes osteoblastic differentiation in primary rat osteoblasts through Smad-Runx2 signaling pathway. Nutr. Metab. (Lond.) *17*, 9.

16. Kumar, S., Boon, R.A., Maegdefessel, L., Dimmeler, S., and Jo, H. (2019). Role of noncoding RNAs in the pathogenesis of abdominal aortic aneurysm. Circ. Res. *124*, 619–630.

17. Baptista, R., Marques, C., Catarino, S., Enguita, F.J., Costa, M.C., Matafome, P., Zuzarte, M., Castro, G., Reis, A., Monteiro, P., et al. (2018). MicroRNA-424(322) as a new marker of disease progression in pulmonary arterial hypertension and its role in right ventricular hypertrophy by targeting SMURF1. Cardiovasc. Res. *114*, 53–64.

18. Takahashi, K., Satoh, M., Takahashi, Y., Osaki, T., Nasu, T., Tamada, M., Okabayashi, H., Nakamura, M., and Morino, Y. (2016). Dysregulation of ossification-related miRNAs in circulating osteogenic progenitor cells obtained from patients with aortic stenosis. Clin. Sci. (Lond.) *130*, 1115–1124.

19. Chowienczyk, P.J. (2015). Aortic stiffness and disease: location is key. Circulation *131*, 1745–1747.

20. Sidloff, D., Stather, P., Dattani, N., Bown, M., Thompson, J., Sayers, R., and Choke, E. (2014). Aneurysm global epidemiology study: public health measures can further reduce abdominal aortic aneurysm mortality. Circulation *129*, 747–753.

21. Wang, S., Zhang, C., Zhang, M., Liang, B., Zhu, H., Lee, J., Viollet, B., Xia, L., Zhang, Y., and Zou, M.H. (2012). Activation of AMP-activated protein kinase α2 by nicotine instigates formation of abdominal aortic aneurysms in mice in vivo. Nat. Med. *18*, 902–910.

22. Li, D.Y., Busch, A., Jin, H., Chernogubova, E., Pelisek, J., Karlsson, J., Sennblad, B., Liu, S., Lao, S., Hofmann, P., et al. (2018). H19 induces abdominal aortic aneurysm development and progression. Circulation *138*, 1551–1568.

23. Cucina, A., Sapienza, P., Corvino, V., Borrelli, V., Mariani, V., Randone, B., Santoro D'Angelo, L., and Cavallaro, A. (2000). Nicotine-induced smooth muscle cell proliferation is mediated through bFGF and TGF-beta 1. Surgery *127*, 316–322.

24. Gargalovic, P.S., Gharavi, N.M., Clark, M.J., Pagnon, J., Yang, W.P., He, A., Truong, A., Baruch-Oren, T., Berliner, J.A., Kirchgessner, T.G., et al. (2006). The unfolded protein response is an important regulator of inflammatory genes in endothelial cells. Arterioscler. Thromb. Vasc. Biol. *26*, 2490–2496.

25. Tsai, S.H., Huang, P.H., Hsu, Y.J., Peng, Y.J., Lee, C.H., Wang, J.C., Chen, J.W., and Lin, S.J. (2016). Inhibition of hypoxia inducible factor-1alpha attenuates abdominal aortic aneurysm progression through the down-regulation of matrix metalloproteinases. Sci. Rep. *6*, 28612.

26. Prins, P.A., Hill, M.F., Airey, D., Nwosu, S., Perati, P.R., Tavori, H., Linton, M.F., Kon, V., Fazio, S., and Sampson, U.K. (2014). Angiotensin-induced abdominal aortic

aneurysms in hypercholesterolemic mice: role of serum cholesterol and temporal effects of exposure. PLoS One *9*, e84517.

27. Robinet, P., Milewicz, D.M., Cassis, L.A., Leeper, N.J., Lu, H.S., and Smith, J.D. (2018). Consideration of sex differences in design and reporting of experimental arterial pathology studies-statement from ATVB council. Arterioscler. Thromb. Vasc. Biol. *38*, 292–303.

28. Davis, F.M., Rateri, D.L., and Daugherty, A. (2014). Mechanisms of aortic aneurysm formation: translating preclinical studies into clinical therapies. Heart *100*, 1498–1505.

29. Lenk, G.M., Tromp, G., Weinsheimer, S., Gatalica, Z., Berguer, R., and Kuivaniemi, H. (2007). Whole genome expression profiling reveals a significant role for immune function in human abdominal aortic aneurysms. BMC Genomics *8*, 237.

30. Tsai, S.H., Huang, P.H., Tsai, H.Y., Hsu, Y.J., Chen, Y.W., Wang, J.C., Chen, Y.H., and Lin, S.J. (2019). Roles of the hypoximir microRNA-424/322 in acute hypoxia and hypoxia-induced pulmonary vascular leakage. FASEB J. *33*, 12565–12575.

31. Gao, J., Yang, T., Han, J., Yan, K., Qiu, X., Zhou, Y., Fan, Q., and Ma, B. (2011). MicroRNA expression during osteogenic differentiation of human multipotent mesenchymal stromal cells from bone marrow. J. Cell Biochem. *112*, 1844–1856.

32. Li, L., Qi, Q., Luo, J., Huang, S., Ling, Z., Gao, M., Zhou, Z., Stiehler, M., and Zou, X. (2017). FOXO1-suppressed miR-424 regulates the proliferation and osteogenic differentiation of MSCs by targeting FGF2 under oxidative stress. Sci. Rep. *7*, 42331.

33. Ignatieva, E., Kostina, D., Irtyuga, O., Uspensky, V., Golovkin, A., Gavriliuk, N., Moiseeva, O., Kostareva, A., and Malashicheva, A. (2017). Mechanisms of smooth muscle cell differentiation are distinctly altered in thoracic aortic aneurysms associated with bicuspid or tricuspid aortic valves. Front. Physiol. *8*, 536.

34. Rosa, A., Ballarino, M., Sorrentino, A., Sthandier, O., De Angelis, F.G., Marchioni, M., Masella, B., Guarini, A., Fatica, A., Peschle, C., et al. (2007). The interplay between the master transcription factor PU.1 and miR-424 regulates human monocyte/macrophage differentiation. Proc. Natl. Acad. Sci. U S A *104*, 19849–19854.

35. Fukuda, H., Aoki, H., Yoshida, S., Tobinaga, S., Otsuka, H., Shojima, T., Takagi, K., Fukumoto, Y., Akashi, H., Kato, S., et al. (2018). Characterization of SMAD2 activation in human thoracic aortic aneurysm. Ann. Vasc. Dis. *11*, 112–119.

36. Freise, C., Kretzschmar, N., and Querfeld, U. (2016). Wnt signaling contributes to vascular calcification by induction of matrix metalloproteinases. BMC Cardiovasc. Disord. *16*, 185.

37. Hecht, E., Freise, C., Websky, K.V., Nasser, H., Kretzschmar, N., Stawowy, P., Hocher, B., and Querfeld, U. (2016). The matrix metalloproteinases 2 and 9 initiate uraemic vascular calcifications. Nephrol. Dial. Transplant. *31*, 789–797.

38. Ruffenach, G., Chabot, S., Tanguay, V.F., Courboulin, A., Boucherat, O., Potus, F., Meloche, J., Pflieger, A., Breuils-Bonnet, S., Nadeau, V., et al. (2016). Role for runt-related transcription factor 2 in proliferative and calcified vascular lesions in pulmonary arterial hypertension. Am. J. Respir. Crit. Care Med. *194*, 1273–1285.

39. Iyer, V., Rowbotham, S., Biros, E., Bingley, J., and Golledge, J. (2017). A systematic review investigating the association of microRNAs with human abdominal aortic aneurysms. Atherosclerosis *261*, 78–89.

40. Yang, L., Dai, J., Li, F., Cheng, H., Yan, D., and Ruan, Q. (2017). The expression and function of miR-424 in infantile skin hemangioma and its mechanism. Sci. Rep. *7*, 11846.

41. Shen, X., Tang, J., Hu, J., Guo, L., Xing, Y., and Xi, T. (2013). MiR-424 regulates monocytic differentiation of human leukemia U937 cells by directly targeting CDX2. Biotechnol. Lett. *35*, 1799–1806.

42. Takagi, K., Yamakuchi, M., Matsuyama, T., Kondo, K., Uchida, A., Misono, S., Hashiguchi, T., and Inoue, H. (2018). IL-13 enhances mesenchymal transition of pulmonary artery endothelial cells via down-regulation of miR-424/503 in vitro. Cell. Signal. *42*, 270–280.

43. Nishibe, T., Dardik, A., Kondo, Y., Kudo, F., Muto, A., Nishi, M., Nishibe, M., and Shigematsu, H. (2010). Expression and localization of vascular endothelial growth factor in normal abdominal aorta and abdominal aortic aneurysm. Int. Angiol. *29*, 260–265.

44. Choke, E., Cockerill, G.W., Dawson, J., Howe, F., Wilson, W.R., Loftus, I.M., and Thompson, M.M. (2010). Vascular endothelial growth factor enhances angiotensin II-induced aneurysm formation in apolipoprotein E-deficient mice. J. Vasc. Surg. *52*, 159–166 e151.

45. Kaneko, H., Anzai, T., Takahashi, T., Kohno, T., Shimoda, M., Sasaki, A., Shimizu, H., Nagai, T., Maekawa, Y., Yoshimura, K., et al. (2011). Role of vascular endothelial growth factor-A in development of abdominal aortic aneurysm. Cardiovasc. Res. *91*, 358–367.

46. Rahman, S.U., Lee, M.S., Baek, J.H., Ryoo, H.M., and Woo, K.M. (2014). The prolyl hydroxylase inhibitor dimethyloxalylglycine enhances dentin sialophoshoprotein expression through VEGF-induced Runx2 stabilization. PLoS One *9*, e112078.

47. Folsom, A.R., Yao, L., Alonso, A., Lutsey, P.L., Missov, E., Lederle, F.A., Ballantyne, C.M., and Tang, W. (2015). Circulating biomarkers and abdominal aortic aneurysm incidence: the atherosclerosis risk in communities (ARIC) study. Circulation *132*, 578–585.

48. Kent, K.C., Zwolak, R.M., Egorova, N.N., Riles, T.S., Manganaro, A., Moskowitz, A.J., Gelijns, A.C., and Greco, G. (2010). Analysis of risk factors for abdominal aortic aneurysm in a cohort of more than 3 million individuals. J. Vasc. Surg. *52*, 539–548.

49. Ashton, H.A., Gao, L., Kim, L.G., Druce, P.S., Thompson, S.G., and Scott, R.A. (2007). Fifteen-year follow-up of a randomized clinical trial of ultrasonographic screening for abdominal aortic aneurysms. Br. J. Surg. *94*, 696–701.

50. Kent, K.C. (2014). Clinical practice. Abdominal aortic aneurysms. N. Engl. J. Med. *371*, 2101–2108.

51. Baxter, B.T., Terrin, M.C., and Dalman, R.L. (2008). Medical management of small abdominal aortic aneurysms. Circulation *117*, 1883–1889.

52. Miyake, T., Miyake, T., Kurashiki, T., and Morishita, R. (2019). Molecular pharmacological approaches for treating abdominal aortic aneurysm. Ann. Vasc. Dis. *12*, 137–146.

53. Estrelinha, M., Hinterseher, I., and Kuivaniemi, H. (2014). Gene expression studies in human abdominal aortic aneurysm. Rev. Vasc. Med. *2*, 77–82.

54. Wilhite, S.E., and Barrett, T. (2012). Strategies to explore functional genomics data sets in NCBI's GEO database. Methods Mol. Biol. *802*, 41–53.

55. Biros, E., Gäbel, G., Moran, C.S., Schreurs, C., Lindeman, J.H., Walker, P.J., Nataatmadja, M., West, M., Holdt, L.M., Hinterseher, I., et al. (2015). Differential gene expression in human abdominal aortic aneurysm and aortic occlusive disease. Oncotarget *6*, 12984–12996.

56. Daugherty, A., Manning, M.W., and Cassis, L.A. (2000). Angiotensin II promotes atherosclerotic lesions and aneurysms in apolipoprotein E-deficient mice. J. Clin. Invest. *105*, 1605–1612.

57. National Research Council (US) Committee for the Update of the Guide for the Care and Use of Laboratory Animals (2011). The National Academies Collection: Reports Funded by National Institutes of Health. Guide for the Care and Use of Laboratory Animals (National Academy of Sciences).

58. Johnston, K.W., Rutherford, R.B., Tilson, M.D., Shah, D.M., Hollier, L., and Stanley, J.C. (1991). Suggested standards for reporting on arterial aneurysms. Subcommittee on reporting standards for arterial aneurysms, ad hoc committee on reporting standards, society for vascular surgery and north American chapter, international society for cardiovascular surgery. J. Vasc. Surg. *13*, 452–458.

59. Satoh, K., Nigro, P., Matoba, T., O'Dell, M.R., Cui, Z., Shi, X., Mohan, A., Yan, C., Abe, J., Illig, K.A., et al. (2009). Cyclophilin A enhances vascular oxidative stress and the development of angiotensin II-induced aortic aneurysms. Nat. Med. *15*, 649–656.